

Feasibility of ^{99m}Tc -MIP-1404 for SPECT/CT Imaging and Subsequent PSMA-Radioguided Surgery in Early Biochemically Recurrent Prostate Cancer: A Case Series of 9 Patients

Daniel Koehler¹, Markus Sauer¹, Susanne Klutmann¹, Ivayla Apostolova¹, Wencke Lehnert¹, Lars Budäus², Sophie Knipper², and Tobias Maurer^{2,3}

¹Department of Diagnostic and Interventional Radiology and Nuclear Medicine, University Medical Center Hamburg–Eppendorf, Hamburg, Germany; ²Martini-Klinik Prostate Cancer Center, University Hospital Hamburg–Eppendorf, Hamburg, Germany; and ³Department of Urology, University Hospital Hamburg–Eppendorf, Hamburg, Germany

This case series evaluated the feasibility of prostate-specific membrane antigen (PSMA)-radioguided surgery (RGS) with ^{99m}Tc -MIP-1404 in recurrent prostate cancer. **Methods:** Nine patients with PSMA-positive lesions on PET/CT received ^{99m}Tc -MIP-1404 (median, 747 MBq; interquartile range [IQR], 710–764 MBq) 17.2 h (IQR, 16.9–17.5 h) before SPECT/CT and 22.3 h (IQR, 20.8–24.0 h) before RGS. **Results:** Seventeen PSMA-positive lesions were detected on PET/CT (median short-axis diameter, 4 mm; IQR, 3–6 mm; median SUV_{max} , 8.9; IQR, 5.2–12.6). Nine of 17 (52.9%) were visible on SPECT/CT (median SUV_{max} , 13.8; IQR, 8.0–17.9). Except for 2 foci, all PET/CT-positive findings demonstrated intraoperative count rates above the background level (median count, 31; IQR, 17–89) and were lymph node metastases. Moreover, PSMA-RGS identified 2 additional metastases compared with PET/CT. Prostate-specific antigen values decreased after RGS in 6 of 9 patients (67%). **Conclusion:** PSMA-RGS with ^{99m}Tc -MIP-1404 identified lymph node metastases in all patients, including 2 additional lesions compared with PET/CT.

Key Words: prostate cancer; biochemical recurrence; PSMA; salvage therapy

J Nucl Med 2023; 64:59–62
DOI: 10.2967/jnumed.122.263892

Prostate-specific membrane antigen (PSMA)-targeted PET/CT has proven to be a highly sensitive and accurate diagnostic tool for the localization of recurrent prostate cancer (PCa), with a significant impact on clinical decision making (1–3). In locally confined recurrent disease, there are various options for salvage therapy (4). PSMA-radioguided surgery (RGS) is a novel technique in which γ -emitting radiotracers are used to identify metastatic soft-tissue lesions intraoperatively with a γ -probe (5,6). ^{99m}Tc -MIP-1404, a small-molecule PSMA inhibitor, was introduced for SPECT/CT imaging (7,8). Studies evaluating its use in RGS are lacking. The presented case series examines the feasibility of PSMA-RGS with

^{99m}Tc -MIP-1404 in patients with positive nodal disease on PSMA PET/CT in early recurrent PCa.

MATERIALS AND METHODS

Between June and September 2021, 9 patients (median age, 62 y; interquartile range [IQR], 61–67 y) received ^{99m}Tc -MIP-1404 before RGS in recurrent PCa with PSMA PET/CT-positive lymph nodes exclusively within the pelvis (median prostate-specific antigen [PSA] level, 0.74 ng/mL; IQR, 0.41–1.54 ng/mL; Supplemental Table 1 [supplemental materials are available at <http://jnm.snmjournals.org>]). Biochemical recurrence was defined as a PSA level of at least 0.2 ng/mL in 2 or more separate measurements at least 6 wk after prostatectomy or at least 2 ng/mL above the PSA nadir after radiotherapy. Except for patient 7 (PSA nadir, 0.3 ng/mL after radiotherapy), all individuals had undergone prostatectomy (interval from primary treatment to RGS: median, 36 mo; IQR, 15–42 mo) (interval from PSMA PET/CT to RGS: median, 36 d; IQR, 26–54 d). The local institutional review board approved this retrospective analysis (2019-PS-09). All patients were informed about the experimental nature of PSMA-RGS and the associated administration of ^{99m}Tc -MIP-1404 and provided written informed consent for the procedure.

PSMA PET/CT Imaging and Analysis

PET/CT scans were performed at different institutions (Supplemental Table 2). Short- and long-axis diameters were measured for each lesion in the axial plane. The SUV_{mean} of the background was calculated from a 10-cm³ spheric region of interest in the gluteus muscle. The SUV_{max} and SUV_{mean} of each lesion were determined with isocontours set at 40% of the maximum. All lesions were analyzed visually using a 4-point scale according to the PROMISE criteria (9).

PSMA SPECT/CT Imaging and Analysis

^{99m}Tc -MIP-1404 (ROTOP Pharmaka GmbH) was produced under the conditions of §13 (2b) of the Arzneimittelgesetz (German Medicinal Products Act; median radioactivity concentration, 212 MBq/mL; IQR, 199–228 MBq/mL; median purity, 95%; IQR, 95.0%–95.5%). Patients received a median dose of 747 MBq (IQR, 710–764 MBq) 17.2 h (IQR, 16.9–17.5 h) before SPECT/CT. Scans were obtained with an AnyScan Trio (Mediso Medical Imaging Systems: patients 1–4 and 6–9) or a Symbia Intevo Bold (Siemens Healthineers: patient 5) (Supplemental Table 3). All lesions encountered on PET/CT were evaluated semiquantitatively on SPECT/CT corresponding to the description for PET/CT. Moreover, a visual 4-point scale according to uptake was applied (none, 0; minimal, 1; moderate, 2; strong, 3).

Received Jan. 25, 2022; revision accepted Jun. 13, 2022.
For correspondence or reprints, contact Daniel Koehler (d.koehler@uke.de).
Published online Jul. 14, 2022.
COPYRIGHT © 2023 by the Society of Nuclear Medicine and Molecular Imaging.

PSMA-RGS and Specimen Preparation

After the injection of ^{99m}Tc -MIP-1404 (22.3 h [IQR, 20.8–24.0 h]), RGS was conducted using a γ -probe (Crystal Probe CXS-SG603; sensitivity maximum, 13,500 cps/MBq; resolution, 14 mm; energy range, 50–511 keV [Crystal Photonics]), and count rates were considered positive if they were at least double the rate of the background as reported previously (6). The template of dissection was based on the preoperative PSMA PET/CT findings, resulting in either a unilateral or a bilateral lymph node dissection. The pathologic work-up of specimens was performed separately according to their region of origin. Also, adjacent tissue without elevated count rates was dissected, resulting in a complete template-based surgical resection. PSA values were determined 1 mo after PSMA-RGS (median, 31 d; IQR, 30–35 d). A complete biochemical response was defined as a PSA decrease below the threshold for biochemical recurrence.

Statistical Analysis

Continuous variables are described with median and IQR. Statistical analyses were conducted with STATA, version 17.0 (STATA Corp.).

RESULTS

Patient-Based Results

Figure 1 shows representative images of positive lesions on preoperative PSMA PET/CT and PSMA SPECT/CT. ^{99m}Tc -MIP-1404 SPECT/CT demonstrated correlates for PET/CT-positive lesions in 6 patients (67%). Lymph node metastases with count rates above the background level were found in all cases. PSA decreased in 6 of 9 patients (67%), meeting the definition of a complete biochemical response in 5 of 9 (56%).

Lesion-Based Imaging Results

Lesion-based information is provided in Table 1. The median short-axis diameter of all lesions was 4 mm (IQR, 3–6 mm), and the median SUV_{max} was 8.9 (IQR, 5.2–12.6). Of 17 findings

identified on PET/CT, 9 (52.9%) were visible on SPECT/CT (median SUV_{max} , 13.8; IQR, 8–17.9). These SPECT/CT-positive lesions showed an increased median SUV_{max} -to-background ratio on PET/CT compared with SPECT/CT-negative lesions (30.8 [IQR, 19.6–42.2] and 13.7 [IQR 9.4–17.2], respectively).

RGS Results and Histologic Correlation

Except for 2 foci (patient 2, proximal left common iliac and intermediate left internal iliac), all PET/CT-positive lesions demonstrated count rates above the background level regardless of their visualization on SPECT/CT (88.2% positive; median count, 31; IQR, 17–89; median count-to-background ratio, 17; IQR, 10–30). The 2 RGS-negative lesions could also not be identified in the histologic workup of the resected tissue. The remaining 15 lesions were PCa-related lymph node metastases, including 3 lymph node conglomerates (patient 1, distal right internal iliac, 3 lymph nodes; patient 4, left internal iliac, 2 lymph nodes; patient 8, distal left internal iliac, 2 lymph nodes). In addition to the PET/CT-positive lesions, 2 additional lymph node metastases were identified during RGS (patient 3: left external iliac; count, 8; count-to-background ratio, 3; long-axis diameter, 6 mm) (patient 6: left external iliac artery; count, 11; count-to-background ratio, 4; long-axis diameter, 2 mm). Three lymph node metastases were positive neither on PSMA imaging nor during RGS and could be identified only on histology (patient 1: right external iliac; 2 lymph nodes; long-axis diameter, 3 mm) (patient 6: left common iliac; 1 lymph node; long-axis diameter; 2 mm). No tissue specimen with negative histology showed an elevated count (specificity, 100%).

To summarize, 24 of 154 resected lymph nodes were PCa metastases. Nineteen were correctly identified on PET/CT (79.2%) and 12 on SPECT/CT (50%). Twenty-one lymph node metastases were localized during RGS (sensitivity, 87.5%).

DISCUSSION

PSMA-RGS with ^{99m}Tc -MIP-1404 was able to identify lymph node metastases in all patients regardless of visualization on SPECT/CT, including lesions with a long-axis diameter of only 2 mm.

Comparable to the results in the presented group, detection rates of ^{99m}Tc -MIP-1404 SPECT/CT in recurrent PCa have been reported to be 50%–60% per patient in cases with low PSA values of less than 1 ng/mL (7,10). Data directly comparing PSMA PET/CT with PSMA SPECT/CT are lacking for ^{99m}Tc -MIP-1404. Detection rates are expected to be lower for SPECT than for PET because of the inferior spatial resolution. Lawal et al. reported that ^{99m}Tc -HYNIC PSMA SPECT/CT was able to identify 62.5% of nodal lesions that were seen on PSMA PET/CT in patients admitted for primary staging or biochemical recurrence (median PSA, 45.2 ng/mL) (11). In the presented case series, ^{99m}Tc -MIP-1404 SPECT/CT detected 52.9% of all PET/CT-positive lesions. The low median PSA of 0.74 ng/mL in the investigated group and the overall small lesion size may be assumed to be the major causes. However, RGS about 22 h after the injection of ^{99m}Tc -MIP-1404 identified lymph node metastases in all cases and could detect 2 additional lesions compared with preoperative PSMA PET/CT. These results are similar to data on RGS with ^{111}In -PSMA-I&T (5) and ^{99m}Tc -PSMA-I&S (6), indicating that PSMA-RGS with ^{99m}Tc -MIP-1404 is feasible using a comparable uptake time. The additional lymph node metastases found during RGS demonstrated lower count rates than most other lesions. A positive correlation of PSMA expression and tumor volume with lesion uptake has been described (12), and a similar relationship may be assumed for the

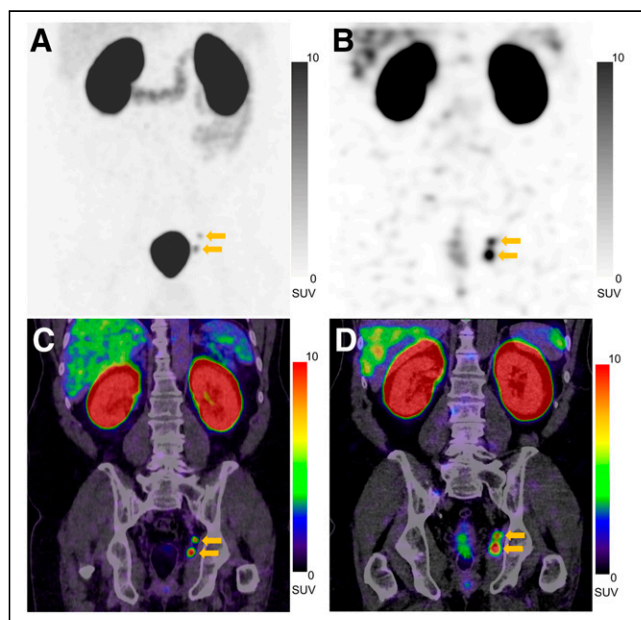


FIGURE 1. ^{68}Ga -PSMA I&T PET/CT (A and C) and ^{99m}Tc -MIP-1404 SPECT/CT (B and D) images of patient 8 (maximum-intensity projections [A and B] and coronal fusion images [C and D]; slice thickness, 3 mm) with PSMA-positive lymph node metastases adjacent to left internal iliac artery (arrows).

TABLE 1
Lesion-Based Case Characteristics

Patient no.	Lesion location	PET/CT					SPECT/CT			RGS		Histology (PCa)
		SAD	LAD	SUV _{max}	SUV _{max} to BG	Visual score	SUV _{max}	SUV _{max} to BG	Visual score	Counts ex vivo (max)	Counts ex vivo (max to BG)	
1	IIR prox.	3	5	8.2	17	2	1.2	3.7	0	54	18	Yes
	IIR dist.	4	5	15.3	31.7	3	9.4	28.8	2	54	18	Yes
2	CIL prox.	2	2	3.6	6	1	1.2	3.5	0	1	1	No
	CIL dist.	4	7	10.5	17.4	3	0.9	2.8	0	8	8	Yes
	IIL prox.	4	5	6.9	11.3	2	1.1	3.1	0	8	8	Yes
	IIL int.	3	4	5.2	8.6	2	1.2	3.5	0	1	1	No
	IIL dist.	4	6	12.6	20.7	3	3.2	9.4	1	17	17	Yes
3	CIL prox.	13	20	5.7	19.6	3	17.9	100.5	3	30	10	Yes
	CIL int.	19	24	9	30.8	3	28.5	160.2	3	31	10	Yes
	CIL dist.	11	28	4.7	16	2	13.8	77.8	3	30	10	Yes
4	IIL	3	5	3.4	10.2	2	0.8	3.8	0	30	10	Yes
5	Pararectal	6	13	3.4	9.3	2	6.7	26.8	2	35	18	Yes
6	IIL	3	5	17.2	35.8	3	1.1	4.6	0	89	30	Yes
7	EIL	11	15	51	114.6	3	112.9	407.6	3	354	118	Yes
8	IIL prox.	2	5	11.4	42.2	3	8	46.3	3	104	35	Yes
	IIL dist.	5	5	15.2	56.3	3	14.8	86.1	3	129	43	Yes
9	Presacral	2	2	8.9	16.1	2	0.8	4.5	0	11	6	Yes

SAD = lesion short axis in mm; LAD = lesion long axis in mm; max = maximum; BG = background; IIR = internal iliac right; prox. = proximal; dist. = distal; CIL = common iliac left; IIL = internal iliac left; int. = intermediate; EIL = external iliac left.

intraoperative count rates. This assumption implies a lower PSMA expression/tumor volume in these lymph nodes, which may have led to their missed visualization on imaging.

Two PET/CT-positive foci with slight tracer uptake in patient 2 could not be found during RGS and were not identified on histopathology. The elevated PSA value after RGS may indicate that the lesions were missed. Alternatively, false-positive results on PET/CT and occult metastases at a different location are possible. Likewise, the PSA values did not decrease in patients 4 and 9 although the PET/CT-positive lymph node metastases were resected successfully. Thus, tumor deposits at other sites that were not detected by preoperative imaging are likely. Follow-up examinations were not available, limiting the interpretation of these cases. Other limitations are the retrospective design, small cohort, and inconsistent PET/CT imaging protocols. Moreover, PSMA-RGS is still an experimental method in which thresholds of intraoperative count rates to differentiate benign from malignant tissues are unclear. As in other metastasis-directed therapies, the clinical utility of PSMA-RGS still has to be determined. Especially, the task of reliably identifying tumor burden in patients with biochemical recurrence to reduce the chance of PSA failure after surgery should be addressed in future studies. However, the large number of correctly identified lymph node metastases by ^{99m}Tc-MIP-1404 RGS is encouraging and should be explored further.

CONCLUSION

PSMA-RGS using ^{99m}Tc-MIP-1404 identified lymph node metastases in all patients with early recurrent PCa regardless of their

visualization on prior SPECT/CT imaging. Thus, ^{99m}Tc-MIP-1404 represents a promising radiotracer for RGS.

DISCLOSURE

No potential conflict of interest relevant to this article was reported.

KEY POINTS

QUESTION: Is RGS with ^{99m}Tc-MIP-1404 feasible in patients with early recurrent PCa?

PERTINENT FINDINGS: RGS with ^{99m}Tc-MIP-1404 discovered PCa-related lymph node metastases in all patients, including 2 additional lesions compared with PET/CT.

IMPLICATIONS FOR PATIENT CARE: RGS with ^{99m}Tc-MIP-1404 is feasible and may represent an alternative to PSMA-RGS with other radiotracers.

REFERENCES

- Fendler WP, Ferdinandus J, Czernin J, et al. Impact of ⁶⁸Ga-PSMA-11 PET on the management of recurrent prostate cancer in a prospective single-arm clinical trial. *J Nucl Med.* 2020;61:1793–1799.
- Calais J, Fendler WP, Eiber M, et al. Impact of ⁶⁸Ga-PSMA-11 PET/CT on the management of prostate cancer patients with biochemical recurrence. *J Nucl Med.* 2018;59:434–441.

3. Emmett L, Tang R, Nandurkar R, et al. 3-year freedom from progression after ^{68}Ga -PSMA PET/CT-triaged management in men with biochemical recurrence after radical prostatectomy: results of a prospective multicenter trial. *J Nucl Med.* 2020;61:866–872.
4. Prostate cancer. European Association of Urology website. <https://uroweb.org/guideline/prostate-cancer/>. Accessed September 22, 2022.
5. Rauscher I, Düwel C, Wirtz M, et al. Value of ^{111}In -prostate-specific membrane antigen (PSMA)-radioguided surgery for salvage lymphadenectomy in recurrent prostate cancer: correlation with histopathology and clinical follow-up. *BJU Int.* 2017;120:40–47.
6. Maurer T, Robu S, Schottelius M, et al. $^{99\text{m}}\text{Tc}$ -based prostate-specific membrane antigen–radioguided surgery in recurrent prostate cancer. *Eur Urol.* 2019;75:659–666.
7. Schmidkonz C, Hollweg C, Beck M, et al. $^{99\text{m}}\text{Tc}$ -MIP-1404-SPECT/CT for the detection of PSMA-positive lesions in 225 patients with biochemical recurrence of prostate cancer. *Prostate.* 2018;78:54–63.
8. Goffin KE, Joniau S, Tenke P, et al. Phase 2 study of $^{99\text{m}}\text{Tc}$ -trofolostat SPECT/CT to identify and localize prostate cancer in intermediate- and high-risk patients undergoing radical prostatectomy and extended pelvic LN dissection. *J Nucl Med.* 2017;58:1408–1413.
9. Eiber M, Herrmann K, Calais J, et al. Prostate Cancer Molecular Imaging Standardized Evaluation (PROMISE): proposed miTNM classification for the interpretation of PSMA-ligand PET/CT. *J Nucl Med.* 2018;59:469–478.
10. Schmidkonz C, Goetz TI, Kuwert T, et al. PSMA SPECT/CT with $^{99\text{m}}\text{Tc}$ -MIP-1404 in biochemical recurrence of prostate cancer: predictive factors and efficacy for the detection of PSMA-positive lesions at low and very-low PSA levels. *Ann Nucl Med.* 2019;33:891–898.
11. Lawal IO, Ankrah AO, Mokgoro NP, Vorster M, Maes A, Sathekge MM. Diagnostic sensitivity of Tc-99m HYNIC PSMA SPECT/CT in prostate carcinoma: a comparative analysis with Ga-68 PSMA PET/CT. *Prostate.* 2017;77:1205–1212.
12. Cytawa W, Kircher S, Kübler H, et al. Diverse PSMA expression in primary prostate cancer: reason for negative [^{68}Ga]Ga-PSMA PET/CT scans? Immunohistochemical validation in 40 surgical specimens. *Eur J Nucl Med Mol Imaging.* 2022;49:3938–3949.